

REDOX BEHAVIOR AND DIFFUSIVITY OF ANTIMONY AND CERIUM ION IN ALKALI ALKALINE EARTH SILICATE GLASS MELTS

KI-DONG KIM, SEUNG-HEUN LEE

Department of Materials Science & Engineering, Kunsan National University, Kunsan 573-701, Chunbuk, Korea

E-mail: kdkim@kunsan.ac.kr

Submitted October 8, 2009; accepted December 21, 2009

Keywords: Antimony and cerium ion, Redox equilibrium, CRT model glass melts, Square wave voltammetry

Redox behavior and diffusivity of antimony and cerium ion in alkali alkaline earth silicate CRT (Cathode Ray Tube) model glass melts were studied by means of square wave voltammetry under the frequency range of 5-1000 Hz and in the temperature range of 800-1400 °C. According to voltammogram, peaks due to Sb^{3+}/Sb^0 were positioned in the negative potential region while peaks due to Sb^{5+}/Sb^{3+} and Ce^{4+}/Ce^{3+} were found in the positive potential region. By using some equations, correlation for peak potential versus temperature and peak current versus reciprocal frequency was examined, respectively. Their correlation showed a linear relation in the applied temperature and frequency range. Based on the linear relationship, thermodynamic and kinetic properties for each redox reaction were suggested.

INTRODUCTION

Most fining chemical agents in glass melts are multivalent ion and undergo following redox reaction through which an electron transfer from one multivalent species to another occurs.



where M is a multivalent ion, n is the number of electrons transferred from one valence state of M to another and electrons are provided or occupied by oxygen during the reaction. Redox reaction of multivalent ion has been studied with the aid of various voltammetry methods [1-15]. Among them square wave voltammetry (SWV) is mainly used to examine the dependence of behavior of multivalent ion on composition and temperature. Russel et al. investigated qualitatively the redox behavior of various multivalent ions in many glass melt systems [1-9] using SWV. In some works there were quantitative approaches determining the ratio of redox couple participating in fining [4, 10] or the self diffusion coefficient of ion [7-9] by SWV.

In the manufacture of cathode ray tube (CRT) glasses consisting of mixed alkali-mixed alkaline earth-silica, the chemical fining is highly important because the glasses as a component of the display device permit virtually no bubble. Antimony oxide is one of the most frequently used chemical fining agents in the CRT glass industry and cerium oxide also contributes to fining of melt. The effectiveness of Sb or Ce in glass melts depends on its valence states, for example Sb^{5+} and Sb^{3+} or

Ce^{4+} and Ce^{3+} under reduction or oxidation atmosphere. According to recent SWV study [15] for CRT glass melt performed at 100Hz, it was found only one peak due to reduction of Sb^{3+} to Sb^0 (expressed as Sb^{3+}/Sb^0) and, no peak for Sb^{5+}/Sb^{3+} and Ce^{4+}/Ce^{3+} in their voltammograms. However, the other SWV studies [6, 7, 9-11, 14] for soda lime silica or alkali borosilicate glass melts containing antimony or cerium showed a peak occurrence for Sb^{5+}/Sb^{3+} and Ce^{4+}/Ce^{3+} in voltammogram and implied the dependence of the peak occurrence on frequency or potential range. This paper provides a further study in extended frequency and potential range on the redox equilibrium for antimony and cerium in alkali alkaline earth silicate CRT glass melts.

EXPERIMENTAL PROCEDURE

Glass preparation

The composition of CRT model glass in mol% is $74.5SiO_2 \cdot 1.4Al_2O_3 \cdot 10RO \cdot 14R'_2O$, in which R is Sr and Ba and R' is Na and K. $0.11Sb_2O_5$ and $0.11CeO_2$ was added as a fining agent, respectively. High-purity raw materials were used to exclude the effect of multivalent impurities. Approximately 300 g of the batch was melted at 1500 °C in a platinum crucible for two hours, and the bubble-free melts were homogenized by stirring of a Pt/Rh rod and transferred to another electric furnace. While the prepared melts were maintained at 1400 °C in the furnace, the electrodes of an electrochemical cell were dipped into the melts to perform the SWV measurement.

Electrochemical cell for SWV measurement consists of three electrodes immersed into the melt in Pt/Rh crucible and potentiostat (Model 273A, EG&G, USA) connected with computer. Platinum plate with 10×20 mm and platinum wire with diameter of 1 mm were used as a counter electrode and a working electrode, respectively. The other platinum wire called reference electrode is connected with O²⁻-conducting Y₂O₃-stabilized ZrO₂ (YSZ) material which is contacted with melts and flushed by reference air with known oxygen partial pressure ($P_{\text{rO}_2} = 0.21$ bar) during SWV experiment. The detailed description for the cell construction is also shown elsewhere [15].

SWV measurements

SWV is for the measurements of current-potential curves under controlled potential consisting of base and step potential, i.e. a definite potential varied with time is applied to a working electrode relative to a reference electrode and the resulting current is registered at the counter electrode. The measured current-potential curve called voltammogram gives valuable information on the behavior of the redox species. For example, if the applied potential is enough to allow electron donation or acceptance between redox species as described in Reaction (1), the resulting voltammogram reveals a characteristic peak current (I_p). The corresponding potential to I_p in voltammogram is called peak potential (E_p) that is equal to the standard potential of the redox pair. Therefore, the equilibrium constant $K(T)$ at temperature T described by using the concentration ($[M^{x+}]$ and $[M^{(x+n)+}]$) of redox pair and the oxygen equilibrium pressure (P_{O_2}) can be expressed in terms of peak potential, E_p , as following Equation (2).

$$K(T) = \frac{[M^{x+}] \cdot P_{\text{O}_2}^{n/4}}{[M^{(x+n)+}]} = \exp \left[\frac{n \cdot F \cdot E_p}{R_g \cdot T} \right] \quad (2)$$

where n is the number of electrons transferred, F is faraday constant and R_g is gas constant. $K(T)$ is also correlated with the standard free enthalpy (ΔG^0), the standard enthalpy (ΔH^0) and the standard entropy (ΔS^0) by following relationship.

$$-R_g T \ln K(T) = \Delta G^0(T) = \Delta H^0 - T\Delta S^0 = -nFE_p \quad (3)$$

The peak current, I_p , depends on the total concentration (C) of the multivalent ion, the diffusion coefficient (D), the peak potential (E_p) and the pulse time (τ) [16],

$$I_p = \frac{0.3n^2 F^2 A \cdot C \cdot E_p}{R_g T} \sqrt{\frac{D}{\pi \cdot \tau}} \quad (4)$$

where A is the surface area of working electrode, F and R_g have their usual meaning.

During SWV measurement at given temperature the furnace was switched off to avoid disturbance of the measured signal by the current of the heating elements. SWV measurements in the present work were performed

under following condition: the range of applied potential and frequency, +200 ~ -800 mV and 5 ~ 1000Hz. The final voltammogram of each melt at the temperature ranging from 1400°C to 1000°C was obtained by subtracting that of the blank melt from the original recorded voltammogram and analyzed with aids of a software.

RESULTS AND DISCUSSION

Figure 1 shows voltammograms at 200 Hz in the temperature range of 1100 ~ 1400 °C recorded in melts doped with 0.11Sb₂O₅. One peak marked by arrow due to the reduction of Sb³⁺ to Sb⁰ is shown at negative potential region and the other peak due to Sb⁵⁺/Sb³⁺ appears clearly at positive potential region. In the case of 0.11CeO₂, as shown in voltammograms of Figure 2 a peak due to Ce⁴⁺/Ce³⁺ is observed only at low temperatures less than 900°C in the present potential range. The corresponding peak potential (E_p) in both Sb and Ce ions moves toward

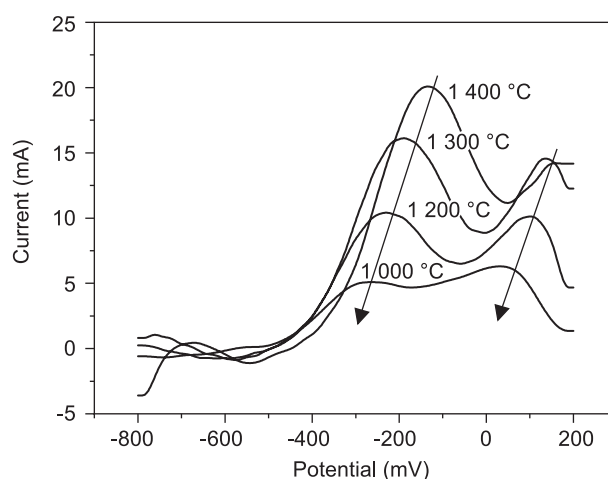


Figure 1. Voltammograms recorded in alkali alkaline earth silicate glass melts doped with 0.11 mol% Sb₂O₅ at 200 Hz.

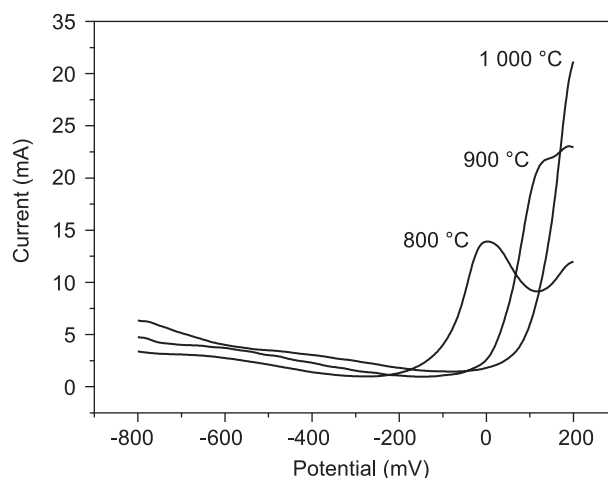


Figure 2. Voltammograms recorded in alkali alkaline earth silicate glass melts doped with 0.11 mol% CeO₂ at 200 Hz.

the negative direction with decrease of temperature, indicating that the equilibrium state of Reaction (1) shifts toward the left, namely to the oxidation state. In Figure 3 the temperature dependence of E_p for Sb^{5+}/Sb^{3+} and Sb^{3+}/Sb^0 is represented. The plot of E_p versus temperature shows a good linearity.

In Figure 4 the logarithm of equilibrium constant ($\ln K$) calculated by Equation (2) is plotted as a function of $1/T$. The temperature dependence of $\ln K$ for Sb^{3+}/Sb^0 and Sb^{5+}/Sb^{3+} shows a good linearity which means that according to equation (3) the reaction enthalpy and

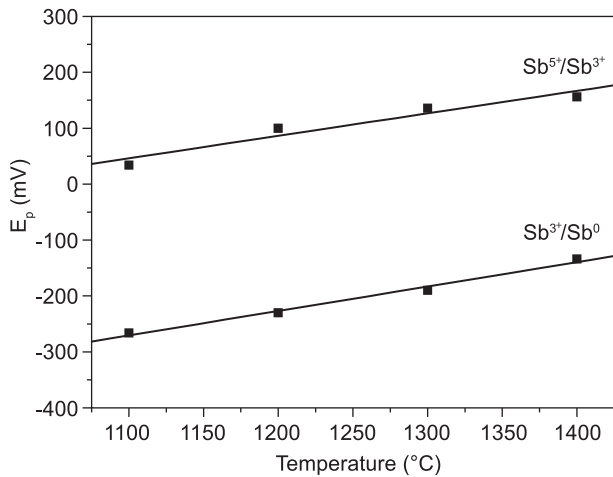


Figure 3. Experimental plots of peak potential (E_p) for Sb^{5+}/Sb^{3+} and Sb^{3+}/Sb^0 as a function of temperature.

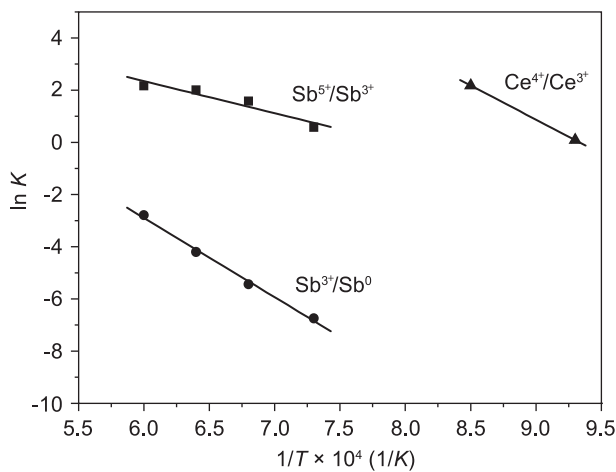


Figure 4. Equilibrium constant ($\ln K$) for Sb^{5+}/Sb^{3+} , Sb^{3+}/Sb^0 and Ce^{4+}/Ce^{3+} as a function of $1/T$.

entropy are temperature independent in the relevant temperature range. In the case of Ce^{4+}/Ce^{3+} , the linearity is also expected although the measured points are only two. The thermodynamic data of redox reaction for Sb^{3+}/Sb^0 , Sb^{5+}/Sb^{3+} and Ce^{4+}/Ce^{3+} were determined by the slope and the interception derived from $\ln K$ versus $1/T$ based on the equation (3). The results for E_p at $1400^\circ C$, ΔH^0 and ΔS^0 for three redox pair were summarized in Table 1. As reported in the literatures [4, 6, 17], the standard free enthalpy (ΔG^0) for both Sb^{5+}/Sb^{3+} and Ce^{4+}/Ce^{3+} in the present melts showed also a negative value unlike the other redox pairs for example Sb^{3+}/Sb^0 , Fe^{3+}/Fe^{2+} , Sn^{4+}/Sn^{2+} and so on. The redox ratio of multivalent ion, $[M^{(x+n)}]/[M^{x+}]$ in glass melts could be calculated using the Equation (2). Table 1 contains the redox ratio and % $[M^{x+}]$ at $1400^\circ C$ in the melts calculated under the assumption that the melt is equilibrated with air ($P_{O_2} = 0.21$ bar). Figure 5 shows the percentages of Sb^{3+} and Sb^0 in investigated temperature range calculated by using following equations. Here K_1 and K_2 denote the equilibrium constant for the reaction of Sb^{5+}/Sb^{3+} and Sb^{3+}/Sb^0 , respectively.

$$\% Sb^{3+} = 100 \frac{[Sb^{3+}]}{[Sb^{3+}] + [Sb^{5+}]} = 100 \frac{K_1(T)}{K_1(T) + 0.21^{1/2}}$$

$$\% Sb^0 = 100 \frac{[Sb^0]}{[Sb^0] + [Sb^{3+}]} = 100 \frac{K_2(T)}{K_2(T) + 0.21^{3/4}}$$

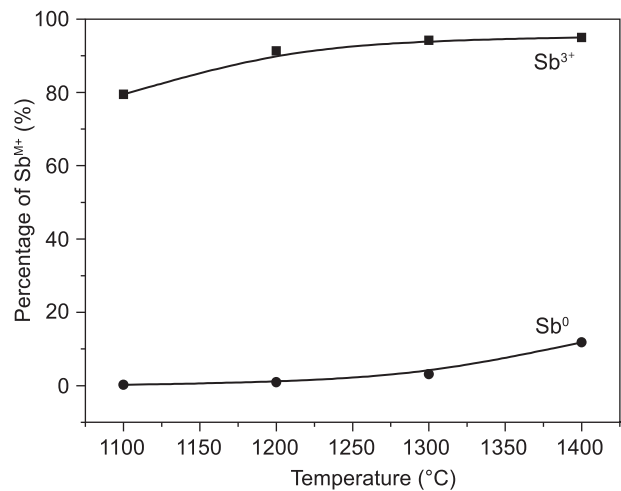


Figure 5. Percentage of Sb^{3+} and Sb^0 as a function of temperature.

Table 1. Peak potentials (E_p), standard enthalpies (ΔH^0), standard entropies (ΔS^0), redox ratios ($M^{(x+n+)}/M^{x+}$) and % (M^{x+}) at $1400^\circ C$.

Redox pair	E_p (mV)	ΔH^0 (kJ/mol)	ΔS^0 (J/molK)	$\log (M^{(x+n+)}/M^{x+})$	% (M^{x+})
Sb^{3+}/Sb^0	-150	252	127	+0.86	12
Sb^{5+}/Sb^{3+}	+160	102	81	-1.28	95
Ce^{4+}/Ce^{3+}	+110 at $900^\circ C$	217	202	-1.12 at $900^\circ C$	93 at $900^\circ C$

The redox ratios, $M^{(x+n+)}/M^{x+}$ and % M^{x+} were calculated using Equation (2) assuming equilibration with air ($=0.21$ bar)

The percentage of antimony in the Sb^{3+} state varies from 95% at 1400 °C to 79 % at 1100 °C while the concentration of metallic antimony (Sb^0) decreases from 12 % to 0.25%. As expected from the temperature dependence of E_p in Figure 3, the percentage of the reduced antimony decreases as the temperature decreases. However, the existence of metallic antimony (which causes a defect in glass products) is scarcely found in the industrial melts of which production is a non-equilibrium process.

In Figures 6a and 6b, voltammograms of the melts containing antimony at 1300 °C and cerium at 900 °C are shown in the frequency range of 5~1000Hz, respectively. E_p values at one temperature were independent of frequency as marked by arrow, namely irrespective of frequency the corresponding peak due to $\text{Sb}^{5+}/\text{Sb}^{3+}$ and $\text{Sb}^{3+}/\text{Sb}^0$ at 1300 °C is located at +125 mV and -200 mV, respectively. However, E_p values for $\text{Ce}^{4+}/\text{Ce}^{3+}$ shows a dependence on frequency. For low frequency of 5 ~

100 Hz, no peak could be observed even within the applied positive potential region. But, at 200 Hz a peak with shoulder type appears at $E_p = +110$ mV and E_p at 1000 Hz comes up to +80 mV. With frequency increase E_p moves toward to direction of negative potential, indicating that at high frequency it is favorable to exist in the form of Ce^{4+} state. Considering that the diffusion coefficient is determined from the slope using the Equation (4), such a dependence of E_p on frequency implies a large diffusion coefficient of Ce^{4+} comparing with constant E_p of antimony ion. The peak current (I_p) in both Figures 6a and 6b show also a great dependence on frequency. According to the relationship between I_p and reciprocal value of square root of pulse time ($\tau^{-1/2}$) as described in Equation (4), a linear correlation is expected under diffusion controlled reaction. In Figure 7a and 7b I_p is plotted as a function of $\tau^{-1/2}$ and a good linear relation is observed. Table 2 contains self-diffusion coefficients (D) of Sb^{5+} , Sb^{3+} , Ce^{4+} calculated from the slope between

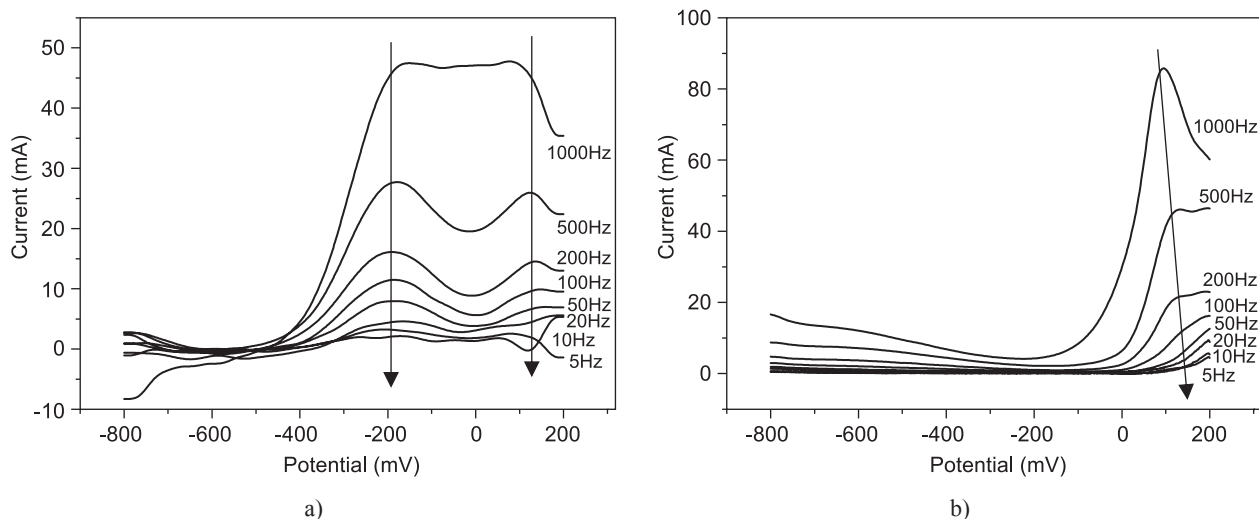


Figure 6. Voltammograms of melts containing: a) antimony at 1300° and b) cerium at 900° in the frequency range of 5 ~ 1000Hz.

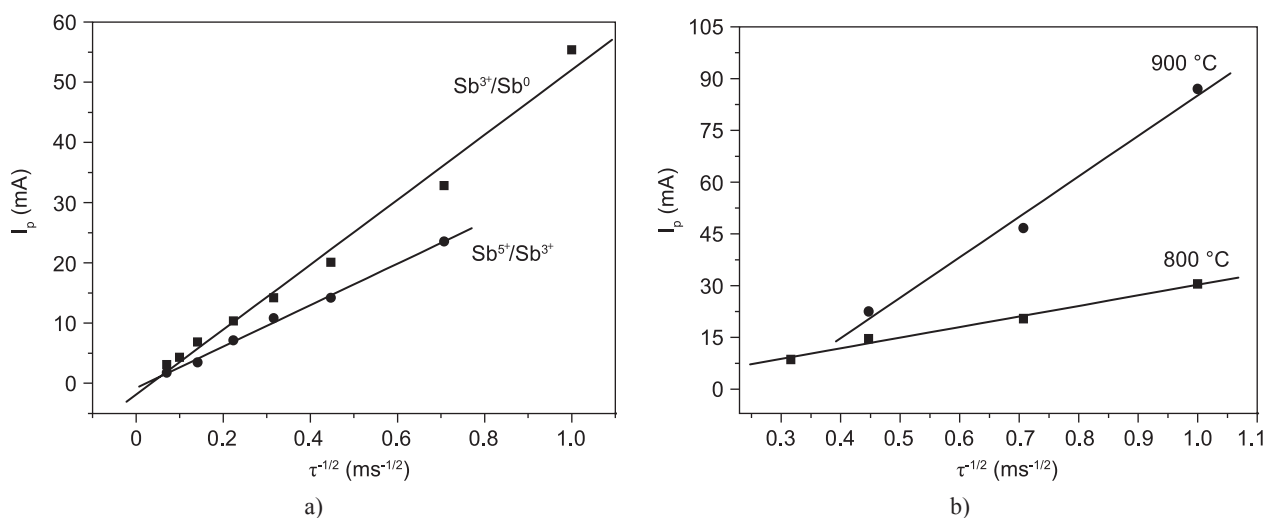


Figure 7. Peak current (I_p) as a function of $\tau^{-1/2}$ for: a) $\text{Sb}^{5+}/\text{Sb}^{3+}$ and $\text{Sb}^{3+}/\text{Sb}^0$ at 1400 °C, b) $\text{Ce}^{4+}/\text{Ce}^{3+}$.

I_p and $\tau^{-1/2}$. Ce^{4+} shows the largest diffusion coefficient among three kinds of ion. $\log D$ of the present melt is plotted as a function of $1/T$ in Figure 8. Within the limits of error, the values can be fitted to an Arrhenius equation, $D = D_0 \exp[-E_D/R_g T]$ where E_D is the activation energy of the self-diffusion process and D_0 the pre-exponential factor. The calculated activation energy, E_D for diffusion was 161 kJ/mol for $\text{Sb}^{5+}/\text{Sb}^{3+}$, 205 kJ/mol for $\text{Sb}^{3+}/\text{Sb}^0$ and 299 kJ/mol for $\text{Ce}^{4+}/\text{Ce}^{3+}$, respectively. Especially, the intersection for antimony ion in Figure 8 indicates that the diffusion coefficient of $\text{Sb}^{3+}/\text{Sb}^0$ is greater than that of $\text{Sb}^{5+}/\text{Sb}^{3+}$ above 1200 °C although $\text{Sb}^{5+}/\text{Sb}^{3+}$ is a dominant reaction at high temperature.

Table 2. Self-diffusion coefficient of antimony and cerium ion.

Temperature (K)	Self diffusivity, D (cm ² /s)		
	$\text{Sb}^{5+}/\text{Sb}^{3+}$	$\text{Sb}^{3+}/\text{Sb}^0$	$\text{Ce}^{4+}/\text{Ce}^{3+}$
1673	5.618×10^{-9}	1.378×10^{-8}	-
1573	9.135×10^{-9}	9.232×10^{-9}	-
1473	3.725×10^{-9}	2.596×10^{-9}	-
1373	8.837×10^{-10}	1.072×10^{-9}	-
1173	-	-	8.570×10^{-6}
1073	-	-	4.912×10^{-7}

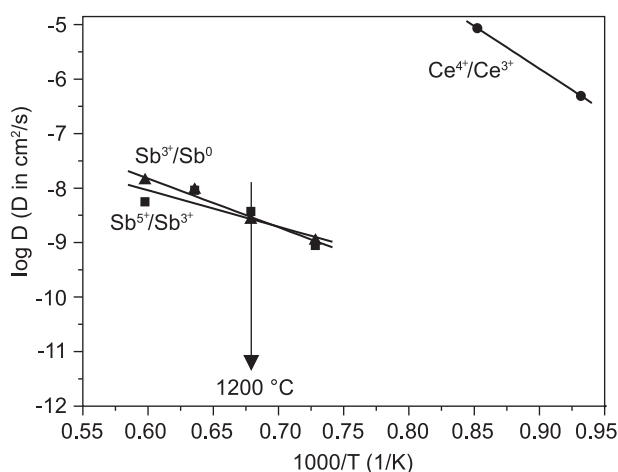


Figure 8. Variation of ions concentration in SBF, in case of G3, with different soaking times.

CONCLUSIONS

For alkali alkaline earth silicate CRT model glass melts containing Sb_2O_5 and CeO_2 square wave voltammetry measurements were performed in the range of applied potential and frequency, +200 ~ -800 mV and

5 ~ 1000 Hz. The resulting voltammograms showed that the reduction peaks due to $\text{Sb}^{5+}/\text{Sb}^{3+}$ and $\text{Ce}^{4+}/\text{Ce}^{3+}$ appeared in the positive potential range while the peaks due to $\text{Sb}^{3+}/\text{Sb}^0$ took place in the negative potential range. Although the peak potential (E_p) for $\text{M}^{x+n}/\text{M}^x$ is normally independent of frequency, E_p values for $\text{Ce}^{4+}/\text{Ce}^{3+}$ showed a dependence on frequency. The thermodynamic properties were calculated based on the temperature dependence of the peak potential. In the case of $\text{Sb}^{5+}/\text{Sb}^{3+}$ and $\text{Ce}^{4+}/\text{Ce}^{3+}$, their standard free enthalpy (ΔG^0) lay in a negative value. The redox ratio in the melts was also calculated using the equilibrium constant and the resulting percentage of the reduced antimony showed a decrease with the temperature decrease. The relationship between peak current and root of frequency showed linearity from whose slope the diffusion coefficients for $\text{Sb}^{5+}/\text{Sb}^{3+}$, $\text{Sb}^{3+}/\text{Sb}^0$ and $\text{Ce}^{4+}/\text{Ce}^{3+}$ were determined.

Acknowledgement

This work was supported by the Korea Science and Engineering Foundation (KOSEF) grant funded by the Korea government (MOST) (No. R01-2006-000-10252-0).

References

- Rüssel C., Freude E.: Phys. Chem. Glasses 30, 62 (1989).
- Rüssel C., Sprachmann G.: J. Non-Cryst. Solids 127, 197 (1991).
- Gerlach S., Claussen O., Rüssel C.: J. Non-Cryst. Solids 248, 92 (1992).
- Claussen O., Rüssel C., Matthai A. in: Proceeding of IV ESG Conference on Glass Science and Technology, p.57-64, Ed. Glafo, Vaxjo Sweden, 1997.
- Claussen O., Rüssel C.: Phys. Chem. Glasses 38, 227 (1997).
- Rüssel C., Gönna G.: J. Non-Cryst. Solids 260, 147 (1999).
- Claussen O., Rüssel C.: J. Non-Cryst. Solids 215, 68 (1997).
- Claussen O., Rüssel C.: Solid State Ionics 105, 289 (1998).
- Gönna G., Rüssel C.: J. Non-Cryst. Solids 261, 204 (2000).
- Takahashi K., Miura Y.: J. Non-Cryst. Solids 38 & 39, 527 (1980).
- Tilquin J.: Electrochimica Acta 38, 479 (1993).
- Tilquin J., Duveiller P., Gilbert J., Clares P.: J. Non-Cryst. Solids 224, 216 (1998).
- Nishimura R., Yamashita H., Maekawa T.: J. Ceram. Soc. Japan 111, 723 (2003).
- Pinet O., Phalippou J., Nardo C. D.: J. Non-Cryst. Solids 352, 5382 (2006).
- Kim K. D., Kim Y. H.: J. Non-Cryst. Solids 354, 553 (2008).
- Osteryoung J. G., Osteryoung R. A.: Anal. Chem. 57, 101A (1985).
- Rüssel C., Gönna G.: J. Non-Cryst. Solids 260, 147 (1999).